Liver INTERNATIONAL
OFFICIAL JOURNAL OF THE INTERNATIONAL ASSOCIATION FOR THE STUDY OF THE LIVER

Liver International ISSN 1478-3223

ORIGINAL ARTICLE

Taurine-induced insulin signalling improvement of obese malnourished mice is associated with redox balance and protein phosphatases activity modulation

Ana P. Cappelli*, Claudio C. Zoppi*, Helena C. Barbosa-Sampaio, José M. Costa-Jr., André O. Protzek, Priscila N. Morato, Antonio C. Boschero and Everardo M. Carneiro

Department of Structural and Functional Biology, Institute of Biology, State University of Campinas (UNICAMP), Campinas, SP, Brazil

Keywords
antioxidant enzymes – hydrogen peroxide – liver – PTEN – PTP1B

Correspondence
Dr. Everardo Magalhães Carneiro, Department of Structural and Functional Biology, Institute of Biology, State University of Campinas (UNICAMP), P.O. Box 6109, Campinas, SP, CEP: 13083-865, Brazil
Tel: +55 19 3521 6203
Fax: +55 19 3521 6185
e-mail: emc@unicamp.br

Received 16 January 2013
Accepted 24 July 2013

DOI:10.1111/liv.12291

Abstract

Background & Aims: Obese protein malnourished mice display liver insulin resistance and taurine (TAU) seems to attenuate this effect. The association between early-life malnutrition and hepatic redox balance in diet-induced insulin resistance is unknown. We investigated TAU supplementation effects upon liver redox state and insulin signalling in obese protein malnourished mice. *Methods:* Weaned male C57BL-6 mice were fed a control (14% protein – C) or a protein-restricted diet (6% protein – R) for 6 weeks. Afterwards, mice received a high-fat diet (34% fat – HFD) for 8 weeks (CH – RH). Half of the HFD-mice were supplemented with TAU (5%) throughout the treatment (CHT – RHT). Body and tissues' weight, respiratory quotient (RQ), glucose tolerance and insulin sensitivity, hepatic oxidant and antioxidant markers and insulin cascade proteins were assessed. *Results:* Protein restriction leads to typical features whereas HFD was able to induce a catch-up growth in RH. HFD-groups showed higher energy intake and adiposity, lower energy expenditure and altered RQ. Glucose tolerance and insulin sensitivity were impaired in HFD-groups and TAU attenuated these effects. H_2O_2 content was increased in CHT and RHT despite no differences in antioxidant enzymes and GSH concentration. AKT and PTEN phosphorylation were significantly increased in CHT but not in RHT. *Conclusion:* Our data provide evidence for an association between TAU-induced improved glycaemic control because of PTEN inactivation and higher AKT phosphorylation. These effects seem to be related with altered hepatic redox balance in obese mice, and this effect is impaired by protein malnutrition.

Liver is one of the major organs regarding blood glucose homeostasis control. Under conditions of increased glucose availability, it is stored as glycogen, whereas during fasting conditions, glycaemia levels could be maintained by releasing liver glucose into the bloodstream.

During post-prandial condition, elevated blood glucose clearance is regulated by insulin. The classical pathway by which insulin exerts its effect is through the binding to the insulin receptor (IR), activating phosphatidylinositol 3-kinase (PI3-K)-protein kinase B (Akt) pathway. The phosphorylation cascade triggered by insulin binding to its receptor seems to be modulated by redox state (1, 2). It was reported that insulin binding to IR stimulates reactive oxygen species (ROS), namely H_2O_2, production that may act as a second messenger in the insulin cascade (3). The notion that hydrogen peroxide (H_2O_2) exerts insulin-like effects was previously described showing that incubation with H_2O_2 resulted in increased glucose uptake in skeletal muscle and adipose tissue (4, 5). Although several insulin cascade proteins have been proposed to be targets of redox modulation (2, 6), the family of protein phosphatases, mainly the tyrosine phosphatases appears as main candidate. In this sense, the protein tyrosine phosphatase 1B (PTP1B) and the phosphatase and tensin homologue (PTEN) are highlighted as main targets of insulin signalling redox control, as they are thiol-dependent enzymes, regulated by the cellular redox state (1, 2, 6, 7).

Early-life malnutrition as well as high-fat diet (HFD)–induced obesity, are known to induce hepatic insulin resistance (8, 9). Despite several other alterations, both conditions were reported to alter intracellular redox balance by increasing ROS production and/or

*These authors contributed equally to this work.

reducing antioxidant capacity, leading to glucose control impairment (10, 11).

On the other hand, it has been reported that taurine (TAU), a sulphur-containing amino acid, that is found in very high concentration in mammalian tissues possesses a variety of biological actions, such as ion movement, antioxidant capacity, osmoregulation and mitochondrial function (12–15). Moreover, TAU was reported to improve insulin secretion and sensitivity in malnourished and obese rodents (16, 17), although the mechanisms are still not completely understood. In this sense, we hypothesize that TAU may exert its action in these models also by modulating the intracellular redox status.

Considering that early-life malnutrition followed by HFD is a common outcome in developing countries, a phenomenon that is in line with epidemiological data of increased obesity, metabolic syndrome and diabetes incidence in these countries (18, 19), we aimed to investigate the effects of this nutritional behaviour upon liver insulin signalling cascade redox control. In addition, we tested the effect of TAU supplementation upon insulin action in the liver of these models. Our hypothesis was that protein malnourished mice followed by HFD-induced obesity would favour hepatic insulin resistance by altering cellular redox balance and TAU supplementation might attenuate this effect.

Material and methods

All the experiments described herein were approved by the State University of Campinas Committee for Ethics in Animal Experimentation and performed according to the 'Principles of laboratory animal care' (NIH publication no. 85-23, revised 1985).

Animals and diet

Male *C57BL/6* mice (21-day-old) from the breeding colony at UNICAMP were housed at 24°C on a 12 h light/dark cycle at the department animal facilities. Mice were maintained in collective cages (four per cage), and randomly assigned into six groups and treated for 105 days as follows: Control group (C) – received diet containing 14% protein throughout the treatment (105 days); Control + HFD (CH) – received diet containing 14% protein for 45 days and afterwards received HFD (34% of fat) for 60 days; Control + HFD + TAU (CHT) – received diet containing 14% protein for 45 days and afterwards received HFD (34% of fat) for 60 days and was also supplemented with TAU. TAU supplementation started immediately after weaning and was supplied in the drinking water (5%); Protein restrict group (R) – received diet containing 6% of protein throughout the treatment (105 days); Protein-restricted + HFD (RH) – received diet containing 6% of protein for 45 days and afterwards received HFD (34% of fat) for 60 days; Protein restrict + HFD + TAU (RHT) – received diet containing 6% of protein for 45 days and afterwards received HFD (34% of fat) for 60 days and was also supplemented with TAU. TAU supplementation started immediately after weaning and was supplied in the drinking water (5%). Mice were weighted weekly throughout the treatment (105 days).

Diets were prepared according to AIN-93 guidelines (20) for adult rodents, with the aforementioned macronutrients alterations.

Food intake

During the last week of the treatment, animals remained in metabolic cages and food intake was measured. We obtained the total food intake/animal's weight ratio and correspondent energy intake was calculated in Kcal per day.

Indirect calorimetry

Before data collection, mice were allowed a 2 h acclimation to the system. After that, animals remained at rest in sealed metabolic cages during light period between 14 and 18 h. O_2 and CO_2 were measured by Oxylet system (Pan Lab/Harvard Instruments, Barcelona, Spain). Respiratory quotient (RQ) was calculated from these data using the Metabolism® software (Pan Lab/Harvard Instruments, Barcelona, Spain) coupled to the system.

Blood samples collection and measurements

Blood samples were collected from the tail for *in vivo* experiments or after decapitation in heparinized tubes. Plasma and serum were obtained by centrifugation at 3000 rpm, respectively, at 4°C, for 12 min. Samples were then stored at −80°C, unless otherwise stated. Plasma total protein was measured using specific kit PROtal (Laborlab, Guarulhos, Brazil). Glycaemia was measured in whole blood using the hand held glycosimeter Accu-Check Advantage II (Roche Ltd., Basel, Switzerland). Plasma insulin concentration was measured by RIA using rat insulin as standard, ^{125}I-labelled bovine insulin was used as the radioactive tracer and guinea-pig anti-porcine insulin serum used as the antibody (21). Aspartate (AST) and alanine (ALT) aminotransferases levels were measured in fresh serum samples with spectrophotometer using specific kits (Laborclin, Pinhais, Brazil) following manufacturer's guidelines.

Intraperitoneal glucose tolerance test (ipGTT) and intraperitoneal insulin tolerance test (ipITT)

IpGTT and ipITT were conducted in different days separated by 1 week, as previously described (22). Briefly, for the ipGTT mice were maintained in a fasted state for 8 h. Previously to 2 g/kg of a 50% (w/v) glucose solution injection was administrated intraperitoneally,

fasting glycaemia was measured (time 0). Glycaemia and insulinaemia were measured at 15, 30, 60, 120 and 180 min after glucose infusion. The area under the curve calculation estimated glucose tolerance. For the ipITT, mice remained fasted for 2 h. Before intraperitoneal human insulin (1.5 U/kg) (Eli Lilly, Indianapolis, IN, USA) infusion, blood glucose was measured (time 0). Afterwards, glycaemia was measured at 5, 10, 15, 20, 25 and 30 min. The constant rate for glucose disappearance (kITT) was calculated using the formula $0.693/t_{1/2}$. Glucose $t_{1/2}$ was calculated from the slope of the least-squares analysis of plasma glucose concentrations during the linear decay phase.

Experimental design and sample extraction

For a more physiological approach, to stimulate insulin signalling, rather than an insulin injection, we used an intraperitoneal glucose load (2 g/kg of a 50% [w/v] glucose solution) or the same volume of a saline solution (control) were administrated. Thirty minutes after the injection, which was the glycaemia and insulinaemia peak as observed during IpGTT, mice were culled and liver samples were quickly frozen in liquid nitrogen and stored at −80° until further analysis. After thawing, unless otherwise stated, liver samples were sliced with scissor and placed on ice-cold buffer containing EDTA 10 mM, Trisma base 100 mM, Sodium Pyrophosphate 100 mM, Sodium Fluoret 100 mM, Sodium Orthovanadate 10 mM, PMSF 2 mM, Aprotinine 0.1 mg/ml. After that, samples were homogenized with a Polytron (Kinematica, Lucerne, Switzerland). Protein content was quantified by the method of Bradford (23).

H_2O_2 content measurement

To measure H_2O_2 content, fresh liver samples were maintained in a Krebs-Hepes (KRBH) buffer (containing in mM: 115 NaCl, 10 $NaHCO_3$, 5 KCl, 1 $MgCl_2$, 2.5 $CaCl_2$, 10 Hepes), pH 7.4 at 37° C in the presence of *Amplex Ultra-red* (Invitrogen, Sao Paulo, Brazil) probe and horseradish peroxidase (0.1 U/ml) during 15 min. After that, 100 µL of the supernatant was used to determine the fluorescence intensity at 530 nm excitation and 590 nm emission. Liver H_2O_2 concentration was calculated against a H_2O_2 concentration curve.

Reduced glutathione (GSH) content measurement

GSH was measured photometrically in fresh liver samples using 5,5-dithiobis-2-nitrobenzoic acid (24). Samples values were interpolated from a standard GSH curve.

RNA extraction and quantitative polymerase chain reaction (PCR)

Liver samples were thawed at room temperature and homogenized in TRIzol reagent (Invitrogen) for 30 s. Total RNA was extracted according to the manufacturer's guidelines and quantified by a spectrophotometer. The integrity of RNA was verified by agarose gel electrophoresis. Complementary DNA was prepared using 3 µg of total RNA and a MultScribe ™ reverse

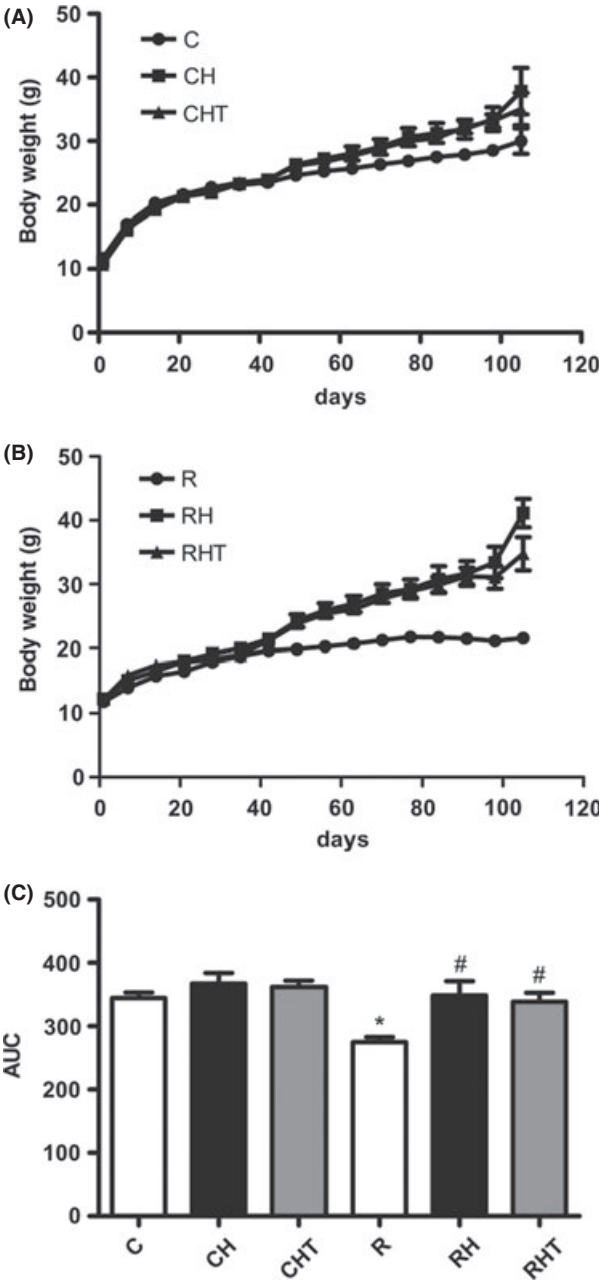

Fig. 1. (A) Body weight of male C57BL/6 mice in control (C), control + high-fat diet (CH) and control + high-fat diet + taurine (CHT). (B) Body weight of male C57BL/6 mice in restricted (R), restricted + high-fat diet (RH) and restricted + high-fat diet + taurine (RHT). (C) Area under the curves referring to graphs A and B (n = 9–13). Values are mean ± SEM. *P < 0.05 vs. control, #P < 0.05 vs. restricted group. One-way ANOVA followed by Tukey.

transcriptase (Applied Biosystems, Foster City, CA, USA). The sequence of the primers is described below and Glyceraldehyde-3-phosphate dehydrogenase (GAPDH) was used as the house-keeping gene. SOD1: Forward 5′-CGTCGGCTTCTCGTCTTGCTCTC Reverse 5′-CACGCACACCGCTTTCATCGC; SOD2: Forward 5′-TGAGGAGAGCAGCGGTCGTGT Reverse 5′-ACGC CGCCCGACACAACATT; GPx1: Forward 5′-GCCGCA CCCTCTTCCCTG Reverse 5′-GTGGCATCGCTTTCTT TCCG; CAT: Forward 5′-GATGAAGCAGTGGAAGGA GC Reverse 5′-TGCCATCTCGTCGGTGAAA; GAPDH: Forward 5′-CCTGCACCACCAACTGCTTA Reverse 5′-GCCCCACGGCCATCACGCCA.

Real-time PCR was carried out in the StepOne cycler (Applied Biosystems). Reactions conditions were 95°C for 10 min, followed by 40 cycles at 95° for 10 s and 60°C for 45 s. Real-time data were analysed using the Sequence Detector System 1.7 (Applied Biosystems).

Western blotting

After samples homogenization, Triton X-100 was added at 1% (v:v) for 30 min. Samples were then centrifuged at 15 000 *g* for 20 min, at 4°C. Equal amounts of proteins of each sample (50 μg) were separated by using 10% SDS-PAGE. After electrophoresis, protein samples were transferred from the gel to a nitrocellulose membrane at 120 V for 90 min. After 2 h blocking in 5% non-fat milk solution at room temperature, immunodetection was performed following an incubation with anti-catalase (Sigma, MO, USA), anti-SOD1 (Abcam, Cambridge, UK), anti-GPx 1 (Abcam), anti-phospho IR (Santa Cruz, CA, USA), anti-phospho AKT (Santa Cruz, CA, USA), anti-phospho PTP1B (Abcam) and anti-GAPDH (Santa Cruz, CA, USA). Membranes were then exposed to 150 ng/ml specific secondary peroxidase-conjugated antibody (anti IgG–HRP, Invitrogen) at room temperature, and visualized by chemiluminescence signal (SuperSignal; Pierce Biotechnology Inc., Rockford, IL, USA) that was detected using a LAS-3000 CCD camera (Fuji, Tokyo, Japan) and quantified by the image J software (ScionCorp., Frederick, MD, USA).

Statistical analysis

Results are expressed as means ± SEM. Statistical analyses were performed with Statistica 6.0 for Windows software (StatSoft, Bedford, UK), using Student's *t*-test and one-way ANOVA with student's Newman–Keuls *post hoc* test. *P* values of less than 0.05 were considered statistically significant.

Results

Growth, nutritional and metabolic parameters

Our protocol of protein malnourishment followed by HFD-induced obesity was successfully reached.

Table 1. Absolute value of body mass, liver, muscle, pancreas, retroperitoneal fat and epididymal fat of C57BL/6 control (C), control + high-fat diet (CH) and control + high-fat diet + taurine (CHT), restricted (R), restricted + high-fat diet (RH) and restricted + high-fat diet + taurine (RHT) treated for 105 days

	C	CH	CHT	R	RH	RHT
Body mass (g)	27.68 ± 0.8	34.42 ± 1.32*,†	31.14 ± 1.11†	21.10 ± 0.59*	29.93 ± 1.03*,†	34.43 ± 0.93*,†
Liver (g)	1.17 ± 0.03	1.26 ± 0.04†	1.28 ± 0.03†	0.78 ± 0.18*	1.01 ± 0.03*,†	1.27 ± 0.07†
Muscle (g)	0.14 ± 0.007	0.16 ± 0.007†	0.15 ± 0.008†	0.11 ± 0.008*	0.15 ± 0.008†	0.15 ± 0.002†
Pancreas (g)	0.18 ± 0.013	0.22 ± 0.017†	0.20 ± 0.013†	0.12 ± 0.011*	0.19 ± 0.02†	0.21 ± 0.015†
Retroperitoneal fat (g)	0.14 ± 0.01	0.40 ± 0.04*,†	0.31 ± 0.03*,†	0.15 ± 0.01	0.37 ± 0.02*,†	0.44 ± 0.04*,†
Epididymal fat (g)	0.42 ± 0.04	1.07 ± 0.12*,†	0.83 ± 0.08*,†	0.37 ± 0.02	1.00 ± 0.09*,†	1.34 ± 0.13*,†

Values represent mean ± SEM, $n = 4–12$.

*Represents a statistical difference compared to the control group, $P < 0.05$ (one-way ANOVA and post test Newman–Keuls).

†Represents a statistical difference compared to the restricted group, $P < 0.05$ (one-way ANOVA and post test Newman–Keuls).

Table 2. Relative value (g/% g body weight) of body mass, heart, liver, muscle, spleen, kidney, pancreas, retroperitoneal fat and epididymal fat of C57BL/6 control (C), control + high-fat diet (CH) and control + high-fat diet + taurine (CHT), restricted (R), restricted + high-fat diet (RH) and restricted + high-fat diet + taurine (RHT) treated for 105 days

	C	CH	CHT	R	RH	RHT
Liver (g)	4.25 ± 0.06	3.67 ± 0.07*	4.15 ± 0.15†	3.73 ± 0.08*	3.39 ± 0.11*	3.70 ± 0.17*
Muscle (g)	0.52 ± 0.02	0.49 ± 0.01	0.49 ± 0.01	0.54 ± 0.03	0.50 ± 0.02	0.46 ± 0.009
Pancreas (g)	0.66 ± 0.04	0.61 ± 0.02	0.66 ± 0.02	0.53 ± 0.01*	0.57 ± 0.02	0.62 ± 0.04
Retroperitoneal fat (g)	0.53 ± 0.05	1.17 ± 0.07*,†	0.75 ± 0.06	0.73 ± 0.06*	1.24 ± 0.06*,†	1.16 ± 0.10*,†
Epididymal fat (g)	1.54 ± 0.14	3.38 ± 0.26*,†	2.84 ± 0.21*,†	1.74 ± 0.08	3.60 ± 0.30*,†	4.00 ± 0.26*,†

Values represent mean ± SEM, $n = 4–12$.

*Represents a statistical difference compared to the control group, $P < 0.05$ (one-way ANOVA, post test Newman–Keuls and "t" student).

†Represents a statistical difference compared to the restricted group, $P < 0.05$ (one-way ANOVA and post test Newman–Keuls).

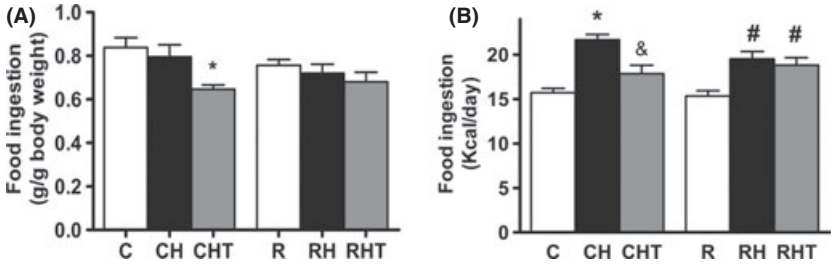

Fig. 2. (A) Food Ingestion (g/g body weight) and (B) calorie intake of male C57BL/6 mice in control (C), control + high-fat diet (CH), control + high-fat diet + taurine (CHT), restricted (R), restricted + high-fat diet (RH) and restricted + high-fat diet + taurine (RHT). (n = 4–6). Values are mean ± SEM. *P < 0.05 vs. control, $^{\#}P$ < 0.05 vs. restricted group. $^{\&}P$ < 0.05 vs. control + high-fat diet. One-way ANOVA followed by Tukey.

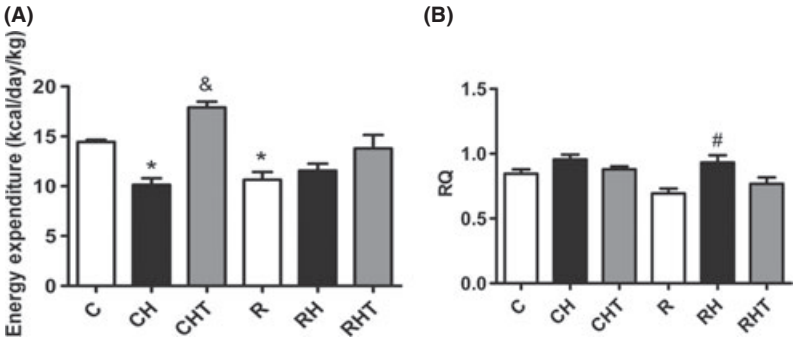

Fig. 3. (A) Respiratory Coefficient and (B) Energy Expenditure of male C57BL/6 mice in control (C), control + high-fat diet (CH), control + high-fat diet + taurine (CHT), restricted (R), restricted + high-fat diet (RH) and restricted + high-fat diet + taurine (RHT). Animals were fed between 21 and 105 days of life. Values are mean ± SEM. *P < 0.05 vs. control. $^{\#}P$ < 0.05 vs. restricted group. $^{\&}P$ < 0.05 vs. control + high-fat diet. One-way ANOVA followed by Tukey.

Table 3. The total protein, triglycerides, cholesterol, AST, ALT, blood glucose and insulin for C56BL/6 mice, control (C), control + high-fat diet (CH) and control + high-fat diet + taurine (CHT), restricted (R), restricted + high-fat diet (RH) and restricted + high-fat diet + taurine (RHT) treated for 105 days

	C	CH	CHT	R	RH	RHT
Total protein fasting (g/dl)	5.6 ± 0.09	5.42 ± 0.09†	5.84 ± 0.23†	4.83 ± 0.32*	5.80 ± 0.17†	5.91 ± 0.17†
Fasting triglycerides (g/dl)	72.37 ± 6.13	65.96 ± 5.17	79.10 ± 5.79	60.97 ± 9.12	72.23 ± 5.31	81.40 ± 5.05
Fasting cholesterol (g/dl)	92.83 ± 7.29	143.2 ± 7.20*,†	119.7 ± 7.65*,†	94.31 ± 4.55	132.7 ± 11.12*,†	129.8 ± 7.22*,†
AST (U/L)	130.9 ± 6.05	151.2 ± 6.03	107.4 ± 23.10	91.05 ± 11.05*	139.1 ± 6.41	104.7 ± 24.98
ALT (U/L)	20.58 ± 1.70	24.83 ± 1.51	28.40 ± 1.43	11.25 ± 2.55*	17.20 ± 2.38	14.17 ± 2.32
Fasting glucose (mg/dl)	81.00 ± 3.96	89.29 ± 5.50*	76.00 ± 4.11	65.22 ± 4.38*	69.88 ± 5.16	87.83 ± 3.81
Fasting insulin (ng/ml)	0.28 ± 0.03	0.91 ± 0.26*,†	0.41 ± 0.15	0.16 ± 0.01*	0.56 ± 0.19	0.43 ± 0.10

Values represent mean ± SEM. Total protein to fast, n = 7–12; triglycerides, n = 7–8; cholesterol tasting, n = 5–10; AST, n = 3–5; ALT, n = 3–5; fasting glucose, n = 4–6; fasting insulin, n = 7–8.

*Represents a statistical difference compared to the control group, P < 0.05 (one-way ANOVA and Tukey post test).

†Represents a statistical difference compared to the restricted group, P < 0.05 (one-way ANOVA and Tukey post test).

Protein-restricted group (R) showed 30% reduced weight gain when compared with C group. HFD increased RH group weight to the same range of normoprotein-fed groups (Fig. 1). Hence, Table 1 shows that several absolute tissues mass; such as skeletal muscle, liver and pancreas, displayed the same pattern among experimental groups; being lower in R and increased until reach control values, after HFD feeding. Interestingly, fat content, analysed here by the epididymal and retroperitoneal fat pads, was not reduced in R. As expected, it was increased after HFD treatment, although remaining at similar levels in all

experimental groups. In a general manner, when absolute tissues weight was normalized by total body mass, this effect was attenuated. However, low-protein-fed tissue values were usually lower than normoprotein-treated mice. HFD treatment increased the values observed in protein-restricted group (RH) to the same range reported in normoprotein-fed groups (CH) (Table 2). Considering the relative tissues weight, it is interesting to note retroperitoneal fat content. R group displayed higher levels of retroperitoneal fat content than C, which might suggest an increased obesity development tendency, induced by protein restriction when followed by HFD treatment. In addition, regarding the aforementioned parameters, our data show that TAU supplementation had no effect in any group, regarding growth parameters.

In agreement with abovementioned effects, Fig. 2 shows that, despite no overall differences were noticed regarding relative food consumption, energy intake was higher in HFD-treated groups. Also interesting of note was that TAU was able to reduce food and consequently energy intake only in CHT, maintaining near to C levels (Fig. 2A and B). Such effect was not observed in RHT group.

In addition to food consumption and energy intake, energy expenditure was significantly lower in R and CH as compared to C values. RH and RHT energy expenditure levels remained at the same low levels reached by R. Nevertheless, TAU was able to increase this parameter in CHT, and despite an observed tendency, it did not exert the same effect in RHT (Fig. 3A). Despite higher fat availability in HFD-treated groups, it was reported a significant increase in RH respiratory quotient value (Fig. 3B), evidencing whole body higher carbohydrate oxidation and probably some level of mitochondrial dysfunction. These effects have been reported in obese insulin resistant and diabetic humans and rodents (25, 26).

In agreement with previous data, plasma variables also reflected dietary treatments (Table 3). Whereas total protein, fasting blood insulin and glucose content were reduced in R, HFD increased these parameters to control levels in RH and RHT. In addition, HFD increased cholesterol levels in both, normoprotein and protein-restricted groups. AST and ALT were significantly lower in protein malnourished mice whereas HFD and TAU supplementation did not alter their levels. These data suggest that blood AST and ALT are not accurate markers of liver impairment susceptibility induced by protein malnutrition.

Glucose metabolism

Glucose metabolism was also altered by our dietary treatments. Whereas protein restriction increased glucose tolerance and insulin sensitivity, HFD reduced these parameters in all groups, as shown by ipGTT and ipITT data (Figs 4 and 5), providing evidence of insulin resistance development. Regarding whole body glucose homeostasis data, TAU was able to restore glucose homeostasis mainly in CHT, whereas its effect in RHT was not as efficient as observed in normoprotein group, showing only an improvement tendency.

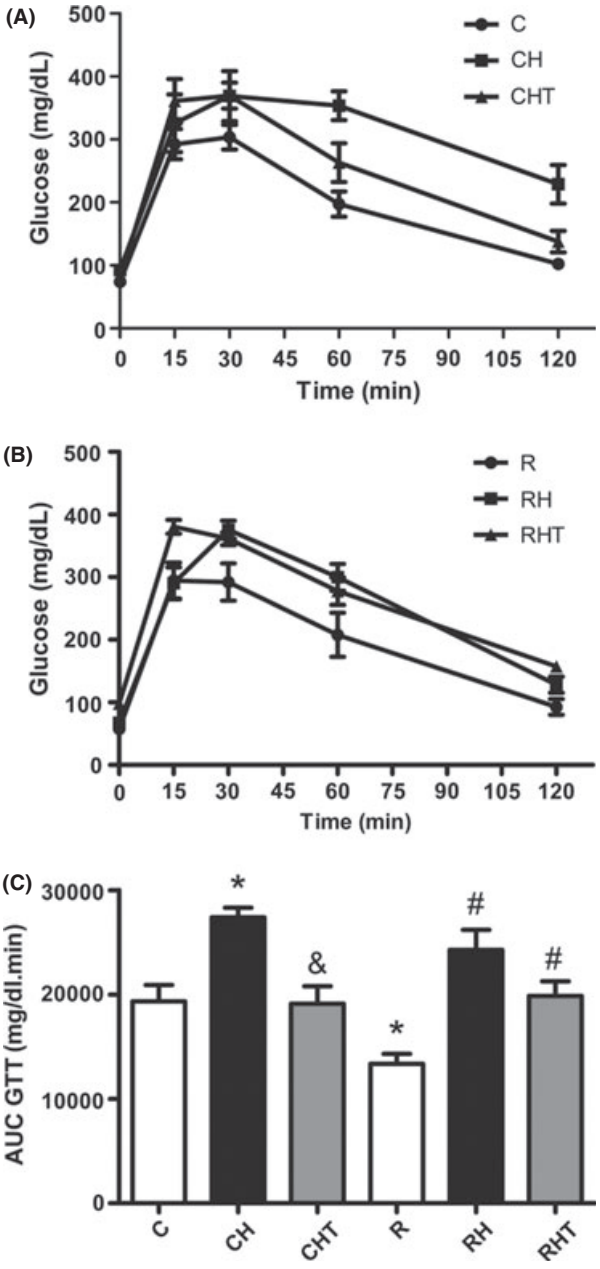

Fig. 4. Intraperitoneal glucose tolerance test (ipGTT). (A) Control (C), control + high-fat diet (CH) and control + high-fat diet + taurine (CHT). (B) Restricted (R), restricted + high-fat diet (RH) and restricted + high-fat diet + taurine (RHT). (C) Area under the curves referring to graphs A and B (n = 5–11). Values are mean ± SEM. $^{*}P < 0.05$ vs. control. $^{\#}P < 0.05$ vs. restricted. $^{\&}P < 0.05$ vs. control + high-fat diet. One-way ANOVA followed by Tukey.

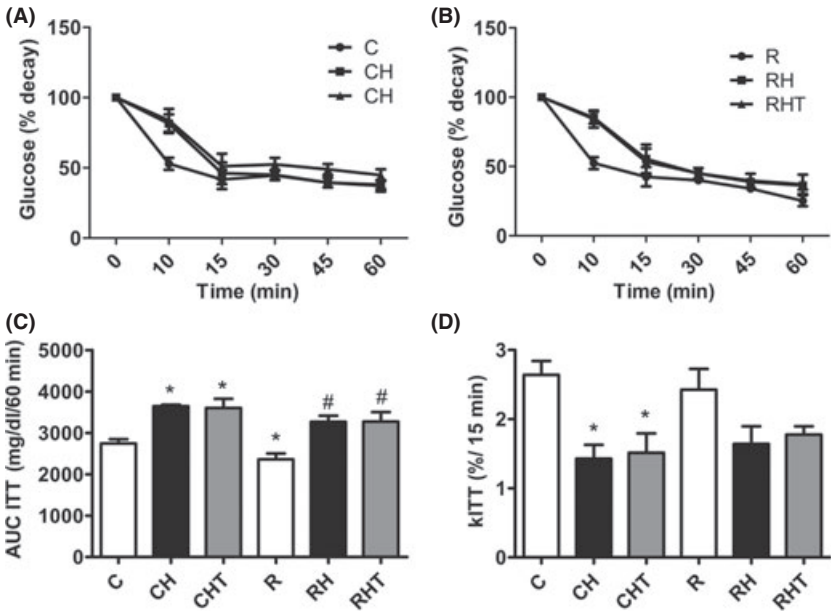

Fig. 5. Intraperitoneal insulin tolerance test (ipITT). (A) Glycaemic curve of male C57BL/6 mice in control (C), control + high-fat diet (CH) and control + high-fat diet + taurine (CHT). (B) Glycaemic curve of male C57BL/6 mice in restricted (R), restricted + high-fat diet (RH) and restricted + high-fat diet + taurine (RHT). (C) Area under the curves referring to the graphs A and B. (D) Percentage of decay of glucose (kITT) in 15 min. (n = 6–12). Values are mean ± SEM. $^{*}P < 0.05$ vs. control. $^{\#}P < 0.05$ vs. restricted. One-way ANOVA followed by Tukey. 'T' student.

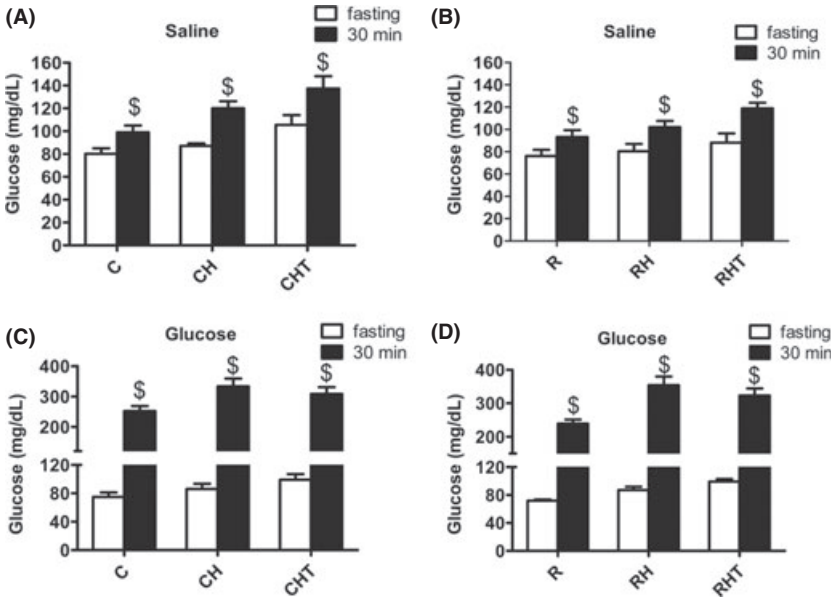

Fig. 6. (A) Fasting plasma glucose and after 30 min of application of saline or (B) 2 g/kg glucose C57BL/6 injection in male C57BL/6 mice. Control (C), control + high-fat diet (CH), control + high-fat diet + taurine (CHT), restricted (R), restricted + high-fat diet (RH) and restricted + high-fat diet + taurine (RHT). (n = 5–11). Values are mean ± SEM. $^{\$}P < 0.05$ vs. the same group in fasting condition. Student's t-test.

Liver redox state and insulin signalling

After the characterization of our experimental models and their effect on blood glucose metabolism, we aimed to investigate liver redox state and insulin signalling. To activate insulin cascade, we used a glucose load (2 g/kg) instead of insulin injection directly, for a more physiological approach. Figure 6 shows that although a slight

blood glucose increase was observed in most groups, when saline was administrated (Fig. 6A and B), glucose load induced a huge increase in blood glucose after 30 min (Fig. 6C and D). In addition, the stimulatory effect of glucose load was clearly demonstrated when we analysed blood insulin content. Whereas saline solution did not change insulinaemia (Fig. 7A and B), glucose load significantly increased blood insulin in all experimental groups (Fig. 7C and D). TAU did not alter blood glucose either insulin levels in any group.

In line with these data, during basal (saline infusion) condition, liver H_2O_2 levels were similar among our experimental groups. However, after the glucose load-stimulated insulin release, we reported increased H_2O_2 production in all groups. Interestingly, both CHT and RHT groups presented higher H_2O_2 content when compared with the other C and R groups, providing a more oxidized environment in hepatocytes within these groups (Fig. 8A and B). As expected, in response to increased H_2O_2 content, GSH levels were lowered to the same extent in all groups (Fig. 9A and B), whereas the main antioxidant (SOD, GPx1 and CAT) enzyme protein levels were, in general, not altered. Exception made to GPx1 in RHT group, which showed a significant increase as compared to R and consequently higher antioxidant capacity induced by TAU supplementation (Fig. 10). These data provide evidence for a transient alteration in the intracellular redox balance after glucose load.

Despite no evidence of increase in the content of insulin cascade-involved proteins, as suggested by unaltered mRNA content from all studied proteins (Table 4), some proteins from insulin signalling pathway displayed altered activities in the liver, specifically in the groups that received TAU supplementation. Whereas low protein and HFD treatment did not induce any significant alterations, TAU supplementation was reported to improve upstream insulin signalling cascade, regardless of glucose load (Fig. 11A and B). Although no alterations were observed in pIR and pPTP 1B content (Fig. 11C and D), a significant increase in AKT phosphorylation in CHT group, and a tendency of increase ($P = 0.09$) in RHT group (Fig. 11E and F) were demonstrated. Accordingly, pPTEN presented also significantly increased phosphorylation in both CHT and RHT groups (Fig. 11G and H), and consequently decreased activation in these groups, favouring AKT activation, as shown by our data.

Discussion

Low birth weight, altered growth pattern in infancy or childhood can predispose obesity, insulin resistance and even type 2 diabetes development later in life, mainly when there is an association of weight reduction and catch-up growth (27, 28). In agreement, we recently demonstrated in an animal model that obese protein malnourished mice display altered systemic glucose control (16). Here, we investigated the consequences of early-life protein malnutrition followed by HFD-induced obesity on the redox control of insulin signalling

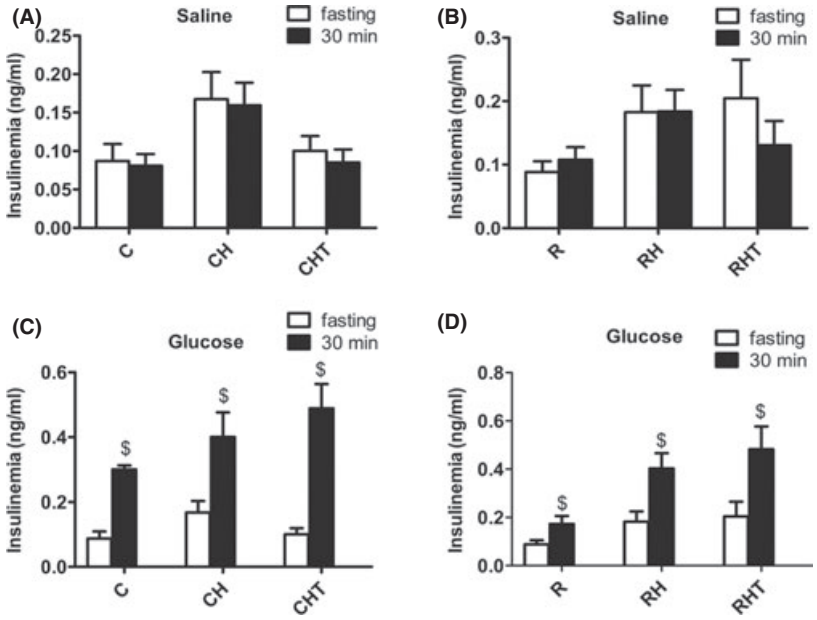

Fig. 7. (A) Fasting plasma insulin and 30 min after application of saline or (B) 2 g/kg glucose in C57BL/6 male mice. Control (C), control + high-fat diet (CH) and control + high-fat diet + taurine (CHT), mice restricted (R), restricted + high-fat diet (RH) and restricted + high-fat diet + taurine (RHT). (n = 4–11). Values are mean ± SEM. $ Represents a statistical difference compared to the baseline group of animals that received the same diet (Student's t-test.).

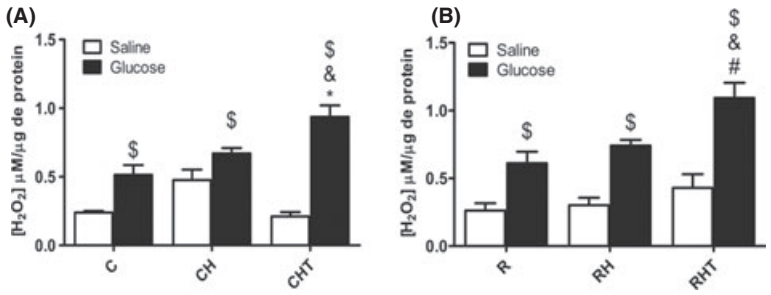

Fig. 8. H_2O_2 concentration in the liver of male C57BL/6. (A) Control (C), control + high-fat diet (CH) and control + high-fat diet + taurine (CHT). (B) Restricted mice (R), restricted + high-fat diet (RH) and restricted + high-fat diet + taurine (RHT). White bars represent animals that received intraperitoneal injection of saline (control) and black bars represent C57BL/6 mice 30 min after glucose load (2 U/kg) (stimulated) (n = 4–9). Values represent mean ± SEM. * Represents a statistical difference in the control group. # Represents a statistical difference in relation to the restricted group. & Represents a statistical difference within the same group that received a high-fat diet without supplementation with taurine $^{\$}P < 0.05$ vs. the same group in saline condition. Student's *t*-test.

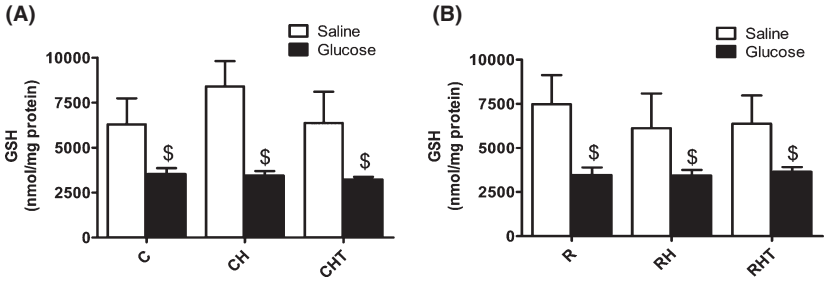

Fig. 9. GSH concentration in the liver of male C57BL/6 mice. (A) Control (C), control + high-fat diet (CH) and control + high-fat diet + taurine (CHT). (B) Restricted mice (R), restricted + high-fat diet (RH) and restricted + high-fat diet + taurine (RHT). White bars represent animals that received intraperitoneal injection of saline (control) and black bars represent C57BL/6 mice 30 min after glucose load (2 U/kg) (stimulated) (*n* = 4–10). Values represent mean ± SEM. $ Represents a statistical difference compared to the baseline group of animals that received the same diet (test 't' student).

in the liver as well as the effect of TAU supplementation on these markers.

As expected, our data revealed that obese protein malnourished mice displayed a reduction in body weight, followed by a catch-up growth. In agreement with literature data, these changes were accompanied by increased adipose tissue deposition and blood lipids content, lower fat oxidation and energy expenditure, leading to whole body glucose tolerance and insulin sensitivity impairment (29, 30). Furthermore, in line with several other reports (31, 32), our protocol of TAU supplementation had no effect upon body weight and fat content, however, it contributed to reducing food intake and increasing energy expenditure, enhancing fat oxidation, as well as improving glucose tolerance and insulin sensitivity mainly in normoprotein-fed, but also in protein-restricted obese mice. Even though we analysed, here only, whole body glucose metabolism by the GTT and ITT, we focused on the liver insulin signalling as it appears as a main organ in glycaemia homeostasis. In addition, our group demonstrated that the same models lead to liver insulin resistance, evidenced by increased glucose output, an effect that was reversed by TAU (16).

As previously stated, insulin signalling cascade seems to be modulated by intracellular redox state. In this sense, low birth weight as well as HFD-induced obesity has been described to alter hepatic redox balance by increased free radical production and/or reduced antioxidant capacity (33, 34). However, the alterations in the fine-tune redox control of insulin signalling specifically in obese malnourished mice have not been addressed.

In opposite to the aforementioned works, our data of H_2O_2 and antioxidant enzymes content did not reveal evidence for an oxidative stress situation in most of our experimental groups. In contrast to the damaging high levels of free radicals, small amounts of these species are recognized as intracellular signalling molecules. It was demonstrated that under physiological conditions, H_2O_2 is needed to start intracellular insulin action; this effect was called the redox priming (35). Similar to the results observed in adipocytes, where high glucose concentration was able to induce increase in H_2O_2 levels, then enhancing insulin signalling (36), our results show that increased blood glucose was associated with higher levels of H_2O_2 and reduced GSH content in the liver.

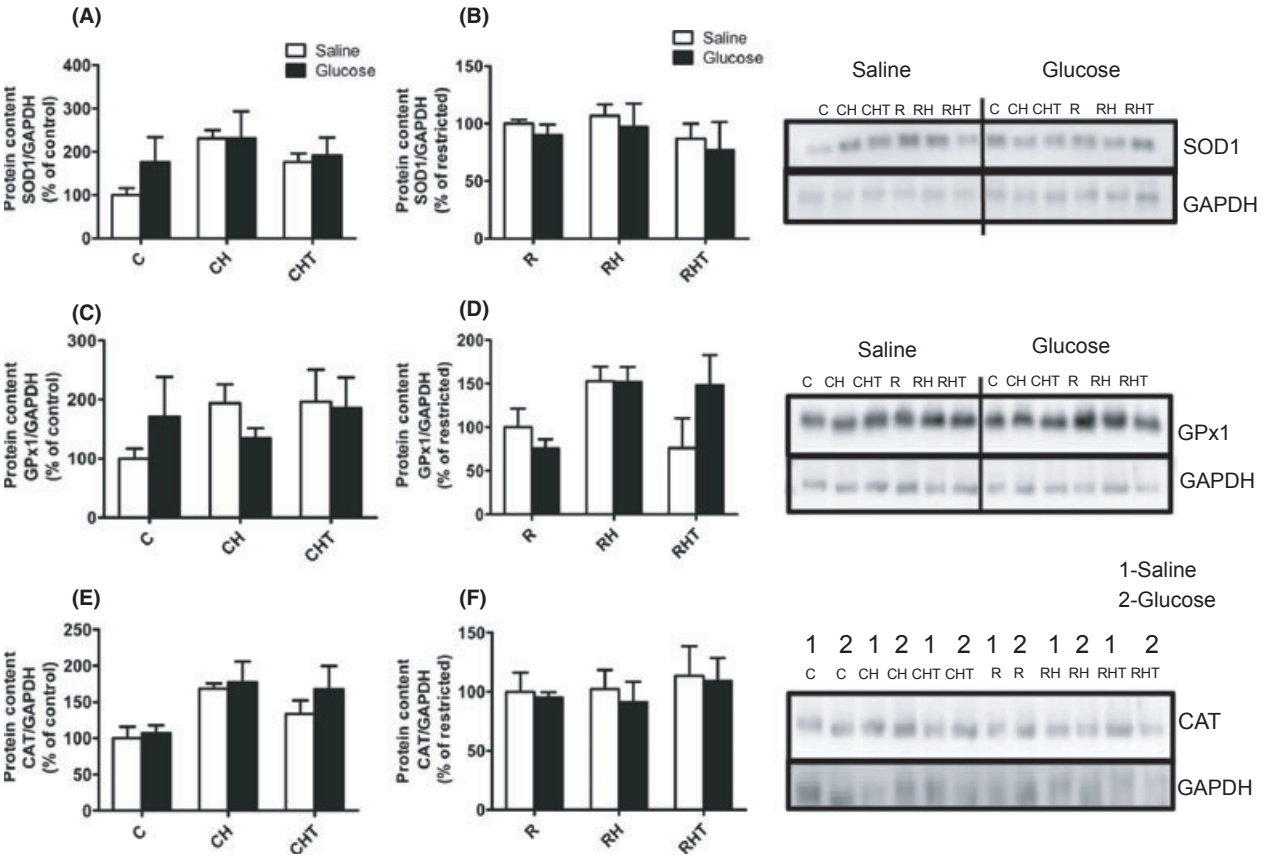

Fig. 10. Protein content of the liver main antioxidant enzymes. (A and B) SOD1, (C and D) GPx1 and (E and F) CAT in C57BL/6 mice. Control (C), control + high-fat diet (CH) and control + high-fat diet + taurine (CHT), restricted (R), restricted + high-fat diet (RH) and restricted + high-fat diet + taurine (RHT) 30 min after the application of saline (white bars) or glucose (black bars) (n = 3–4). Values represent mean ± SEM. (one-way ANOVA and Tukey post test).

Table 4. Gene expression of SOD1, SOD2, CAT, GPxl, IR and AKT liver of mice C56BL/6 control (C), control + high-fat diet (CH) and control + high-fat diet + taurine (CHT), restricted (R), restricted + high-fat diet (RH) and restricted + high-fat diet + taurine (RHT) treated for 105 days

	C	CH	CHT	R	RH	RHT
S0D1/GAPDH	1.00	1.50 ± 0.46	1.09 ± 0.09	1.01 ± 0.17	1.08 ± 0.26	1.16 ± 0.15
SOD2/GAPDH	1.00	1.56 ± 0.34	1.16 ± 0.07	0.97 ± 0.10	1.18 ± 0.12	1.29 ± 0.14
CAT/GAP H	1.00	1.49 ± 0.27	1.03 ± 0.27	1.06 ± 0.16	1.50 ± 0.02	1.65 ± 0.23
GPxl/GAPDH	1.00	1.42 ± 0.18	1.11 ± 0.14	0.88 ± 0.05	0.99 ± 0.20	0.89 ± 0.07
IR/GAPDH	1.00	1.59 ± 0.22	2.53 ± 0.66	0.94 ± 0.08	1.20 ± 0.21	3.03 ± 0.41*,†
AKT/GAPDH	1.00	1.31 ± 0.17	1.10 ± 0.07	0.97 ± 0.16	1.13 ± 0.09	1.49 ± 0.21

Values represent mean ± SEM. For SOD 1, n = 3–4; SOD 2, n = 3–4; CAT, n = 4; GPx1, n = 3–4; IR, n = 3–4; and Akt, n = 4.
*Represents a statistical difference compared to the restricted group, $P < 0.05$ (one-way ANOVA and Tukey post test).
†Represents a statistical difference within the same group, compared to the group receiving high-fat diet without taurine supplementation, $P < 0.05$ (one-way ANOVA and Tukey post test).

Hence, higher H_2O_2 and GPX1 levels in TAU supplemented groups were detected. Interestingly, a positive relationship between these redox markers and insulin signalling, specifically at PTEN and AKT activation, was found only in TAU supplemented group. As previously proposed, glucose load induced a transient change to a more oxidized environment in the adipocytes and skeletal muscle cells, which seems to be essential for insulin action (4, 5). In this sense, TAU supplementation might favour intracellular redox balance by increasing H_2O_2

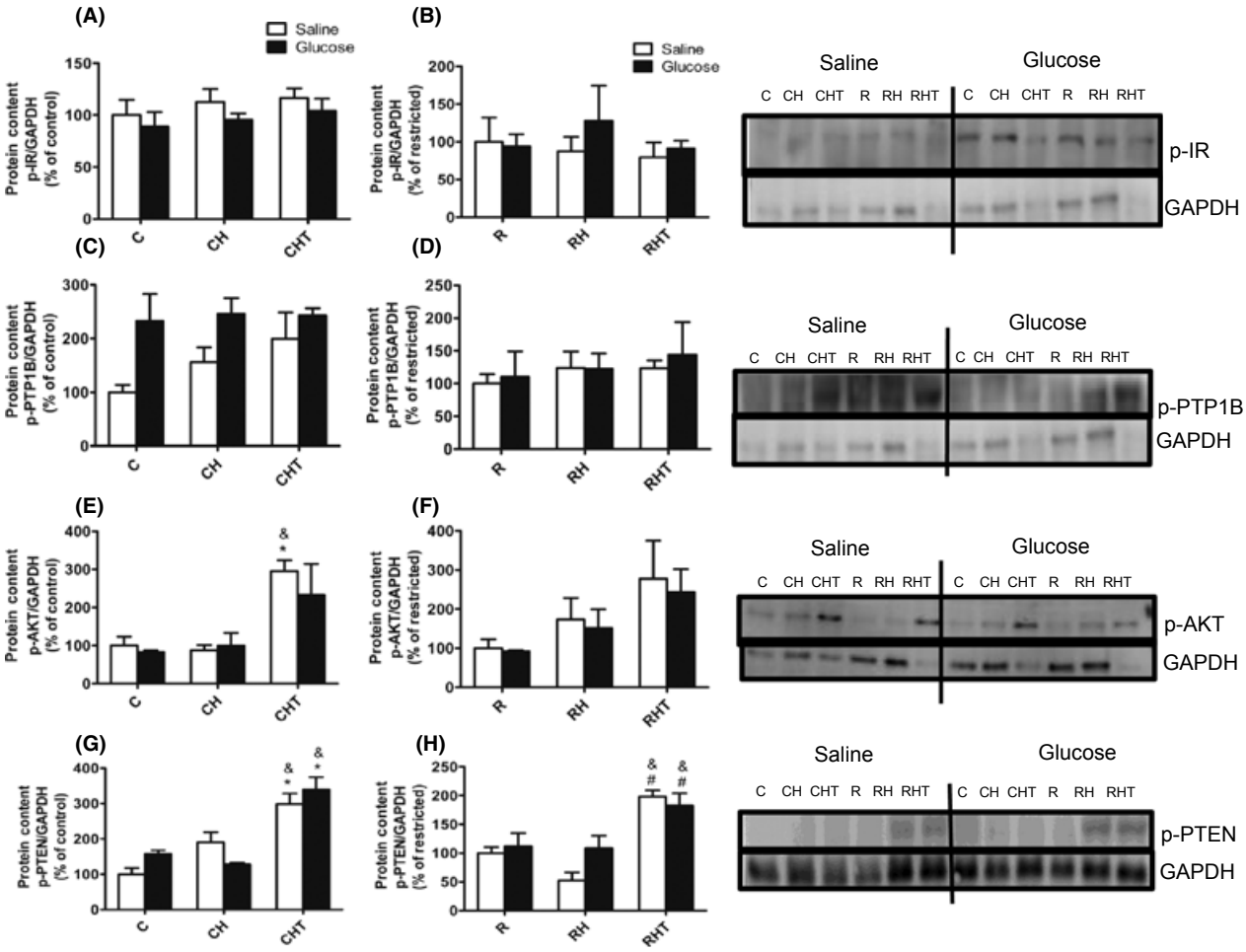

Fig. 11. Liver regulatory insulin cascade proteins phosphorylation. (A and B) p-IR, (C and D) p-PTP1B, (E and F) p-AKT and (G and H) p-PTEN in C57BL/6 mice. Control (C), control + high-fat diet (CH) and control + high-fat diet + taurine (CHT), restricted (R), restricted + high-fat diet (RH) and restricted + high-fat diet + taurine (RHT) 30 min after saline (white bars) or glucose injection (black bars) (n = 3–4). Values represent mean ± SEM. * Represents a statistical difference in the control group. # Represents a statistical difference in relation to the restricted group. & Represents a statistical difference within the same group in the group that received a high-fat diet without supplementation with taurine. $P < 0.05$ (one-way ANOVA and Tukey post test).

production and antioxidant capacity. TAU antioxidant capacity to protect hepatocytes, has already been described (37), however, the mechanism involved in the improved H_2O_2 production, as showed by our results, needed to be further investigated. Thus, an increased TAU content might favour hepatocytes redox balance and insulin signalling in our HFD-treated mice.

Regarding insulin signalling modulation, several kinases and phosphatases have been proposed as candidates of the redox control of insulin action (2). PTP1B and PTEN are pointed as the main phosphatases involved in insulin cascade that are regulated by the redox state. For instance, PTP1B and PTEN were described to be involved with insulin resistance in obese mice (38, 39). PTP1B and PTEN counteract insulin effects by removing the phosphates from IR, insulin receptor 1(IRS1) and PI3K respectively (1, 2, 40). On the other hand, H_2O_2 oxidizes the catalytic cysteine tiol of these enzymes reducing their affinity for their substrates, allowing enhanced insulin signal transduction. Although several studies described the association between PTP1B and insulin resistance in HFD-treated models, suggesting this enzyme as a possible therapeutic target against metabolic syndrome (41), our results did not show any alterations in PTP1B and IR phosphorylation in the liver from obese mice. However, AKT and PTEN phosphorylation were significantly increased when TAU was supplemented, mainly in CHT and to a lesser extent in RHT. Whereas AKT phosphorylation increases its activity, the same effect impairs PTEN binding to membrane reaching the active conformation (42) removing its capacity to inactivate PI3K. Thus, reduced PTEN activity may allow the observed increase in AKT activation and insulin signal transduction in the liver then, favour-

ing improved glucose tolerance and insulin sensitivity in TAU supplemented mice.

In conclusion, our data provide evidence for an association between TAU-induced improved liver insulin signal transduction and enhanced whole body glucose tolerance because of alterations in hepatic redox balance in obese mice. In addition, early-life protein malnutrition seems to impair these TAU effects. However, the mechanisms by which this impairment occurs need to be established.

Acknowledgements

Financial support: FAPESP, CNPq, National Institute of Obesity and Diabetes (NICTOD) and CEPID grants are acknowledged here.

Conflict of interest: The authors do not have any disclosures to report.

References

1. Bashan N, Kovsan J, Kachko I, Ovadia H, Rudich A. Positive and negative regulation of insulin signaling by reactive oxygen and nitrogen species. *Physiol Rev* 2009; **89**: 27–71.
2. Goldstein BJ, Mahadev K, Wu X, Zhu L, Motoshima H. Role of insulin-induced reactive oxygen species in the insulin signaling pathway. *Antioxid Redox Signal* 2005; **7**: 1021–31.
3. Mahadev K, Motoshima H, Wu X, *et al.* The NAD(P)H oxidase homolog Nox4 modulates insulin-stimulated generation of H2O2 and plays an integral role in insulin signal transduction. *Mol Cell Biol* 2004; **24**: 1844–54.
4. Mukherjee SP, Lynn WS. Role of cellular redox state and glutathione in adenylate cyclase activity in rat adipocytes. *Biochim Biophys Acta* 1979; **568**: 224–33.
5. Higaki Y, Mikami T, Fujii N, *et al.* Oxidative stress stimulates skeletal muscle glucose uptake through a phosphatidylinositol 3-kinase-dependent pathway. *Am J Physiol Endocrinol Metab* 2008; **294**: E889–97.
6. de Keizer PL, Burgering BM, Dansen TB. Forkhead box o as a sensor, mediator, and regulator of redox signaling. *Antioxid Redox Signal* 2011; **14**: 1093–106.
7. Monteiro HP, Arai RJ, Travassos LR. Protein tyrosine phosphorylation and protein tyrosine nitration in redox signaling. *Antioxid Redox Signal* 2008; **10**: 843–89.
8. Feres NH, Reis SR, Veloso RV, *et al.* Soybean diet alters the insulin-signaling pathway in the liver of rats recovering from early-life malnutrition. *Nutrition* 2010; **26**: 441–8.
9. Lalli CA, Pauli JR, Prada PO, *et al.* Statin modulates insulin signaling and insulin resistance in liver and muscle of rats fed a high-fat diet. *Metabolism* 2008; **57**: 57–65.
10. Begriche K, Massart J, Robin MA, Bonnet F, Fromenty B. Mitochondrial adaptations and dysfunctions in nonalcoholic fatty liver disease. *Hepatology* 2013. Early view.
11. Spoelstra MN, Mari A, Mendel M, *et al.* Kwashiorkor and marasmus are both associated with impaired glucose clearance related to pancreatic beta-cell dysfunction. *Metabolism* 2012; **61**: 1224–30.
12. Hansen SH, Andersen ML, Cornett C, Gradinaru R, Grunnet N. A role for taurine in mitochondrial function. *J Biomed Sci* 2010; **17**(Suppl. 1): S23.
13. Ito T, Pastukh V, Solodushko V, Azuma J, Schaffer SW. Effect of taurine on protein kinase C isoforms: role in taurine's actions? *Adv Exp Med Biol* 2009; **643**: 3–11.
14. Schaffer SW, Azuma J, Mozaffari M. Role of antioxidant activity of taurine in diabetes. *Can J Physiol Pharmacol* 2009; **87**: 91–9.
15. Militante JD, Lombardini JB, Schaffer SW. The role of taurine in the pathogenesis of the cardiomyopathy of insulin-dependent diabetes mellitus. *Cardiovasc Res* 2000; **46**: 393–402.
16. Batista TM, Ribeiro RA, da Silva PM, *et al.* Taurine supplementation improves liver glucose control in normal protein and malnourished mice fed a high-fat diet. *Mol Nutr Food Res* 2012; **57**: 423–34.
17. Batista TM, Ribeiro RA, Amaral AG, *et al.* Taurine supplementation restores glucose and carbachol-induced insulin secretion in islets from low-protein diet rats: involvement of Ach-M3R, Synt 1 and SNAP-25 proteins. *J Nutr Biochem* 2012; **23**: 306–12.
18. Fagot-Campagna A. Emergence of type 2 diabetes mellitus in children: epidemiological evidence. *J Pediatr Endocrinol Metab* 2000; **13**(Suppl. 6): 1395–402.
19. Silva AA, Santos CJ, Amigo H, *et al.* Birth weight, current body mass index, and insulin sensitivity and secretion in young adults in two Latin American populations. *Nut Metab Cardiovasc Dis* 2012; **22**: 533–9.
20. Reeves PG, Rossow KL, Lindlauf J. Development and testing of the AIN-93 purified diets for rodents: results on growth, kidney calcification and bone mineralization in rats and mice. *J Nutr* 1993; **123**: 1923–31.
21. Scott AM, Atwater I, Rojas E. A method for the simultaneous measurement of insulin release and B cell membrane potential in single mouse islets of Langerhans. *Diabetologia* 1981; **21**: 470–5.
22. Filiputti E, Rafacho A, Araujo EP, *et al.* Augmentation of insulin secretion by leucine supplementation in malnourished rats: possible involvement of the phosphatidylinositol 3-phosphate kinase/mammalian target protein of rapamycin pathway. *Metabolism* 2010; **59**: 635–44.
23. Bradford MM. A rapid and sensitive method for the quantitation of microgram quantities of protein utilizing the principle of protein-dye binding. *Anal Biochem* 1976; **72**: 248–54.
24. Faure P, Lafond JP. Measurement of plasma sulphydryl and carbonyl groups as a possible indicator of protein oxidation. In: Favier AE, ed. *Analysis of Free Radicals in Biological Systems*. Basel: Birkhauser Verlag, 1995; 237–48.
25. Muoio DM, Noland RC, Kovalik JP, *et al.* Muscle-specific deletion of carnitine acetyltransferase compromises glucose tolerance and metabolic flexibility. *Cell Metab* 2012; **15**: 764–77.
26. Galgani JE, Moro C, Ravussin E. Metabolic flexibility and insulin resistance. *Am J Physiol Endocrinol Metab* 2008; **295**: E1009–17.
27. Dulloo AG. Thrifty energy metabolism in catch-up growth trajectories to insulin and leptin resistance. *Best Pract Res Clin Endocrinol Metab* 2008; **22**: 155–71.
28. Dulloo AG, Antic V, Yang Z, Montani JP. Propellers of growth trajectories to obesity and the metabolic syndrome. *Int J Obes* 2006; **30**(Suppl. 4): S1–3.
29. Martins VJ, Toledo Florencio TM, Grillo LP, *et al.* Long-lasting effects of undernutrition. *Int J Environ Res Public Health* 2011; **8**: 1817–46.

30. Dunger DB, Salgin B, Ong KK. Session 7: early nutrition and later health early developmental pathways of obesity and diabetes risk. *Proc Nutr Soc* 2007; **66**: 451–7.
31. Solon CS, Franci D, Ignacio-Souza LM, *et al.* Taurine enhances the anorexigenic effects of insulin in the hypothalamus of rats. *Amino Acids* 2012; **42**: 2403–10.
32. Harada N, Ninomiya C, Osako Y, *et al.* Taurine alters respiratory gas exchange and nutrient metabolism in type 2 diabetic rats. *Obes Res* 2004; **12**: 1077–84.
33. Morita M, Ishida N, Uchiyama K, *et al.* Fatty liver induced by free radicals and lipid peroxidation. *Free Radical Res* 2012; **46**: 758–65.
34. Fetoui H, Garoui M, Zeghal N. Protein restriction in pregnant- and lactating rats-induced oxidative stress and hypohomocysteinaemia in their offspring. *J Anim Physiol Anim Nutr* 2009; **93**: 263–70.
35. Schmid E, Hotz-Wagenblatt A, Hacj V, Droge W. Phosphorylation of the insulin receptor kinase by phosphocreatine in combination with hydrogen peroxide: the structural basis of redox priming. *FASEB J* 1999; **13**: 1491–500.
36. Wu X, Zhu L, Zilbering A, *et al.* Hyperglycemia potentiates H(2)O(2) production in adipocytes and enhances insulin signal transduction: potential role for oxidative inhibition of thiol-sensitive protein-tyrosine phosphatases. *Antioxid Redox Signal* 2005; **7**: 526–37.
37. Das J, Ghosh J, Manna P, Sil PC. Acetaminophen induced acute liver failure via oxidative stress and JNK activation: protective role of taurine by the suppression of cytochrome P450 2E1. *Free Radical Res* 2010; **44**: 340–55.
38. Meshkani R, Adeli K. Hepatic insulin resistance, metabolic syndrome and cardiovascular disease. *Clin Biochem* 2009; **42**: 1331–46.
39. Garcia-Ruiz I, Solis-Munoz P, Gomez-Izquierdo E, *et al.* Protein-tyrosine phosphatases are involved in interferon resistance associated with insulin resistance in HepG2 cells and obese mice. *J Biol Chem* 2012; **287**: 19564–73.
40. Stoker AW. Protein tyrosine phosphatases and signalling. *J Endocrinol* 2005; **185**: 19–33.
41. Bence KK. Hepatic PTP1B deficiency: the promise of a treatment for metabolic syndrome? *J Clin Metab Diabetes* 2010; **1**: 27–33.
42. Ross AH, Gericke A. Phosphorylation keeps PTEN phosphatase closed for business. *Proc Natl Acad Sci USA* 2009; **106**: 1297–8.